

Biosorption of Acid Orange 7 (AO7) dye by canola waste: equilibrium, kinetic and thermodynamics studies

Davoud Balarak^{a,*}, Hajar Abasizadeh^b, Jae-Kyu Yang^c, Moo Joon Shim^d, Seung-Mok Lee^{d,*}

^aDepartment of Environmental Health, Health Promotion Research Center, Zahedan University of Medical Sciences, Zahedan, Iran, email: dbalarak2@gmail.com (D. Balarak)

^bStudent Research Committee, Zahedan University of Medical Sciences, Zahedan, Iran, email: hajarabasizadeh@gmail.com (H. Abasizadeh)

^cDepartment of Environmental Engineering, Kwangwoon University, Seoul, Korea, email: jkyang@kw.ac.kr (J.-K. Yang)

^dDepartment of Environmental Engineering, Catholic Kwandong University, Gangneung 25601, Korea, emails: moojoonshim@gmail.com (M.J. Shim), leesm@cku.ac.kr (S.-M. Lee)

Received 16 August 2019; Accepted 9 February 2020

ABSTRACT

In order to study the availability of canola residue for biosorption of acid orange 7 (AO7) from aqueous solution, batch experiments were performed for thermodynamic and kinetic studies. Physical characterization of canola samples was determined by Fourier transform infrared spectroscopy, scanning electron microscopy, X-ray diffraction, and Brunauer–Emmett–Teller. The equilibrium adsorption data were analyzed using Langmuir and Freundlich isotherms. Langmuir isotherm was well fitted with the experimental adsorption data. Kinetic analysis were performed using pseudo-first order, pseudo-second-order and intra-particle diffusion models. The kinetic analysis indicated that the adsorption kinetic data of AO7 fit better to the pseudo-second-order kinetic model. In addition, the existence of three steps were observed during the adsorption experiment. The first stage represented the transport of AO7 molecules from the surface to pores of the adsorbent external structure. The second stage showed invasion of the molecules into the internal structure of the adsorbent. The adsorption of the molecule on the interior surface of the adsorbent was the last step. The thermodynamic data obtained at different temperatures were used to calculate standard free energy changes (ΔG°), standard enthalpy change (ΔH°), and standard entropy change (ΔS°). All ΔG° values are ranged from -4.987 to -0.045 kJ/mol; ΔH° and ΔS° values of canola biomass were 29.62 kJ/mol and 0.107 J/mol K, respectively. Based on the calculation, adsorption of AO7 onto canola biomass was a spontaneous and endothermic process.

Keywords: Adsorption; Canola residue; Kinetic; Acid Orange 7; Thermodynamics

1. Introduction

Synthetic dyes in wastewaters are from various industrial sources (e.g., textile, leather, cosmetics, paper, electronics, printing, plastic, pharmaceutical, food, etc) [1,2]. Anionic azo dyes contain many compounds from various classes of dyes. Acid Orange 7 (AO7) used in special areas such as leather dyeing and paper coloration [3]. Like most other azo dyes,

it tends to be disposed of in industrial wastewater and poses a severe health threat to humans. It is highly toxic, and its ingestion can cause eye, skin, mucous membrane, and upper respiratory tract irritation; severe headaches; nausea; water-borne diseases [4].

As the synthetic dyes are toxic with the wastewaters many harmful and carcinogenic chemicals can be transported easily to the other streams and rivers [5]. The discharge of

* Corresponding authors.

dye-bearing wastes without any treatment into the natural streams and rivers not only affects their aesthetic nature but also interferes with the transmission of sunlight and therefore reduces the photosynthetic activity and creates severe problems for the aquatic life, food web [1]. In some cases, the color wastewater can also endure anaerobic removal to form potentially carcinogenic compounds that can end up in the food chain [6].

Therefore, well-controlled management of these wastewaters is required and it is a reasonably vital issue to meet the national discharge standards [7]. There are several techniques (e.g., aerobic or anaerobic digestion, coagulation, advanced oxidation processes and adsorption) to remove the color from wastewaters [8,9]. They are not usually eliminated by conventional methods of wastewater treatment in the wastewater treatment plant because of the complex structure [10].

It has been proven that the adsorption is a highly efficient and relatively low-cost technique for the treatment of wastewaters containing dyes [8,11]. Generally, activated carbon and resin have been commonly used to adsorptive removal of dyes. However, adsorption processes with these materials have some disadvantages, requiring high costs associated with their subsequent treatment and regeneration [12,13].

Thus, this problem leads to the urgent development of novel and cost-effective adsorbents. Recently, various bioadsorbents such as agricultural and animal waste have been applied to remove dyes from wastewaters [14,15]. Since the agricultural adsorbents showed good performance due to having high specific surface area and little internal diffusion resistance, these materials have drawn much attention in recent years. Lignin and cellulose are main constituents in agricultural residues [16,17]. Agricultural residues also include hemicellulose, lipids, proteins, glucose, starch, water, hydrocarbons and other compounds [18,19] which can combine with pollutants by replacing hydrogen ions or by forming complexes with pollutant ions [20].

Canola waste can be considered as a recommendable adsorbent because carboxylic and hydroxyl groups of the canola waste have a great affinity for dye ions [21]. Furthermore, it is inexpensive, abundant and easy to prepare [22,23]. Thus, the main objectives of this study are: (a) to investigate removal capacity of AO7 dye by canola, (b) to determine the influence of factors including contact time, temperature, initial AO7 dye concentration on the dye removal efficiency, and (c) to analyze thermodynamics and kinetics of the adsorption.

2. Materials and methods

AO7 was purchased from Sigma-Aldrich Co., US, and its chemical structure of AO7 is $C_{16}H_{11}N_2NaO_4S$ (molecular weight 350.32 g/mol) (Fig. 1). No purification for AO7 was conducted before the experiments. All AO7 solutions were prepared using deionized water. Canola residue was used as an adsorbent for the removal of AO7 dye from aqueous solutions. The canola stem was taken from the research farm in the Tabriz Agricultural School. Then the taken residues were washed several times with deionized water until dirt particles were washed out. This washing procedure had been

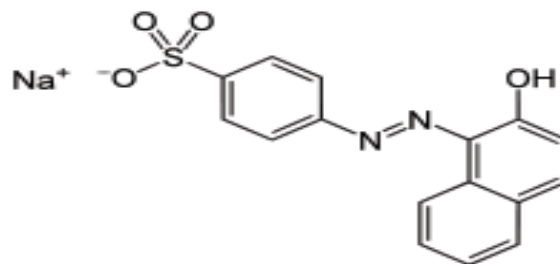


Fig. 1. Chemical structure of AO7.

continued until the washed water was colorless, and then the washed residues were dried at 50°C for 12 h. The dried materials were ground using steel mill and sieved through 1–2 mm sieve. After the ground particles were sieved then they were treated with 0.1 M HCl for 5 h. Next they were washed with deionized water and dried. The final biomass was used in the adsorption process in this study.

2.1. Characterization of dried canola biomass

An ASAP 2000 apparatus was used to determine the specific surface area of canola, and the analysis was based on nitrogen adsorption–desorption isotherms at 77 K. An environmental scanning electron microscopy (ESEM) instrument (Philips XL30 ESEM-TMP, USA) was used to take micrograph of canola biomass before and after adsorption. An X-ray diffraction (XRD) spectrometer (Philips-X'Pert Pro MPD) was used to examine the changes in a crystalline phase, and the conditions of the XRD were following: generator voltage of 40 kV, tube current of 40 mA, scan step size of 0.02°, and the scan range of 5°–90°. To study the interaction between functional groups on the surface of dried canola and AO7, Fourier transform infrared (FT-IR) spectroscopic measurements were conducted using Nicolet 5700 instrument, Thermo Corp., USA, in wavenumbers ranging from 400 to 4,000 cm^{-1} .

2.2. Batch adsorption studies

The stock solution of AO7 (1,000 mg/L) was diluted to prepare initial AO7 solutions with different concentrations. The pH of the initial solutions was adjusted by using 0.1 M H_2SO_4 and 0.1 M NaOH solutions. A specific amount of bioadsorbent was put to a 50 mL polypropylene tube after 20 mL of AO7 solution was added at the desired pH. The tube was stirred at 180 rpm for 90 min at 293 K. The equilibrium times were estimated at four different temperatures (273, 288, 303, and 318 K) when AO7 concentrations in the samples were consistent. When the equilibration time was over, the solution was centrifuged at 3,600 rpm for 10 min to have supernatant. Then it was analyzed for AO7 using a UV-Spectrophotometer (DR-2800) at λ_{max} 452 nm which was obtained in preliminary tests. The content of AO7 on dried canola biomass was calculated by the difference between the initial and final AO7 concentrations in the supernatant. All batch experiments were conducted three times.

The adsorption capacity at the equilibrium, q_e (mg/g), was estimated by Eq. (1) [22]:

$$q_e = \frac{(C_0 - C_e)V}{W} \quad (1)$$

where C_0 and C_e (mg/L) are the liquid-phase concentrations of dye at initial and equilibrium, respectively. V (L) and W (g) represent the volume of the solution and the mass of sorbent used, respectively. The removal percentage of the dye was estimated by Eq. (2) [23]:

$$R = \frac{C_0 - C_e}{C_0} \times 100 \quad (2)$$

2.3. Desorption studies

Desorption of adsorbed AO7 from canola biomass was studied with four types of the solvent including deionized water and different concentrations of sodium chloride (0.1, 0.2 and 0.4 N). Pre-adsorbed canola biomass was taken in 100 ml of the above-mentioned solvent and shaken at 120 rpm for 90 min.

3. Results and discussion

3.1. Characterization

The Brunauer–Emmett–Teller (BET) analysis indicated that the surface area of the treated canola was determined as 72.5 m²/g. Fig. 2 displays the examination of dried canola before and post adsorption using ESEM. Before adsorption, there was the pore textural structure of dried canola. In contrast, clear pore textural structure was not observed after adsorption due to either agglomeration on the surface or the incursion of AO7 into the pores of dried canola. Table 1 represents the chemical compositions of the canola. The canola was mainly composed of the C, O, H, and N of which accounted for 91% of the total weight (w/w). The other minor components were Si (3.6%), K (3.1%), Ca (1.1%), P (0.7%), and Mg (0.5%). XRD patterns of the dried canola (a) before and (b) after adsorption showed a quite similar diffused peak with a maximum at $2\theta = 21.2^\circ$ and 21.5° , respectively (Fig. 3). However, due

to AO7 biosorption, dried canola after adsorption shows a higher intensity on the surface of dried canola. To understand the interaction between functional groups on the surface of the dried canola and AO7, FT-IR analysis was performed before and after adsorption. The FT-IR spectra of the dried canola were not changed, showing a similar pattern and the same number of observed peaks before and after adsorption (Fig. 4).

The overlap of O–H and N–H stretching vibrations resulted in the broad peak at 3,431.1 cm⁻¹, suggesting that surface free hydroxyl groups and chemisorbed water were presented [24]. At 2,918.2 and 1,391.2 cm⁻¹, the peaks showed correspondence to the C–H symmetric stretching vibration of the methylene groups (–CH₂) and deformation vibration of methyl groups (–CH₃). At 1,629.4 cm⁻¹, the peaks attributed to a C=O stretching vibration of carboxylate (–COO–) or N–H deformation vibration of amide I groups. At 1,265 and 1,041 cm⁻¹, the peaks were because of the C–O stretching vibration of ketones, aldehydes and lactones or carboxyl groups [25]. However, some shifts in wavenumbers from 3,431.1 to 3,419.2 cm⁻¹, from 1,629.4 to 1,632.6 cm⁻¹, from 1,265 to 1,271.5 cm⁻¹, and from 1,041 to 1,048.6 cm⁻¹ were attributed to the spectra of dried canola before and after adsorption. This change of wavenumbers indicates the possibility that amide, hydroxyl, carboxylate and C–O groups could participate in AO7 biosorption on the surface of canola [26].

Table 1
Elemental compositions of canola

Sample	%
O	41.4
C	39.6
H	6.6
N	3.4
Si	3.6
K	3.1
Ca	1.1
P	0.7
Mg	0.5

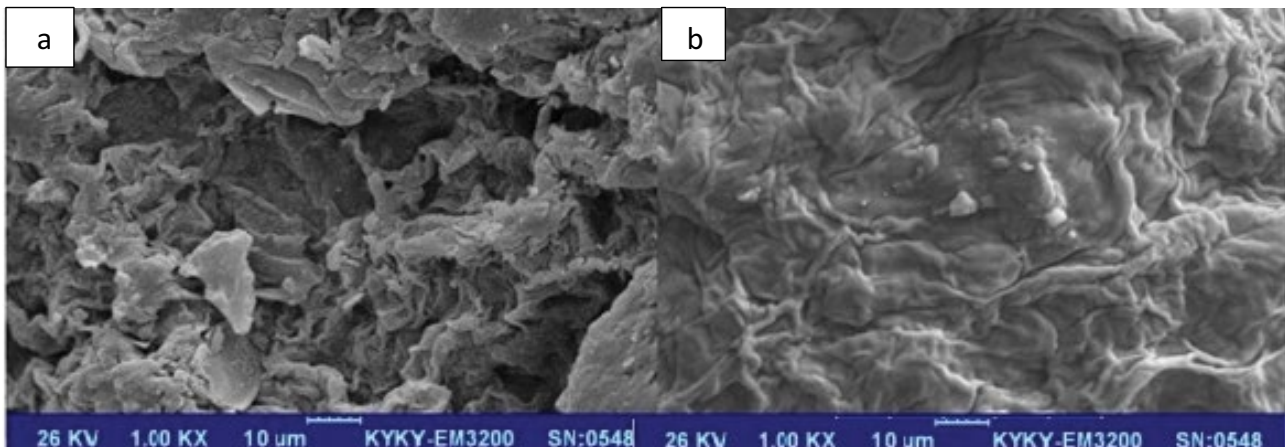


Fig. 2. SEM image of the canola biomass: (a) before and (b) after adsorption.

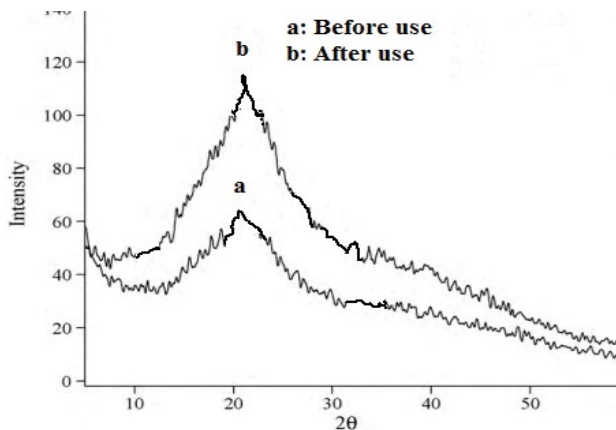


Fig. 3. XRD patterns of the dried canola biomass: (a) before and (b) after adsorption.

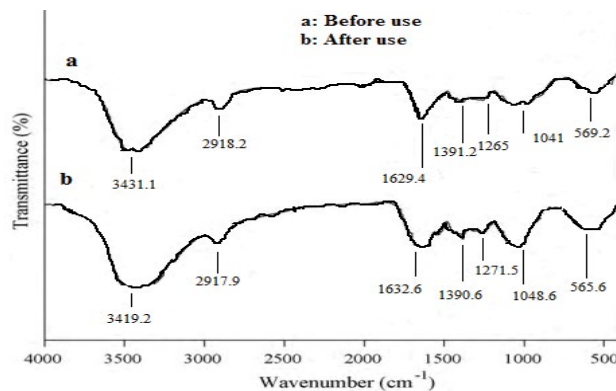


Fig. 4. FT-IR spectrum of the dried canola: (a) before and (b) after adsorption.

3.2. Adsorption isotherms

Fig. 5 displays the adsorption isotherms of AO7 on canola at 273, 293, 313 and 333 K, respectively. As shown in Fig. 5, equilibrium uptake increased with increasing AO7 concentrations. This result indicates that the concentration gradient was the driving force for the adsorption reaction [27]. When the concentration of AO7 increases, the active sites of canola will be surrounded by much more AO7 ions, causing favorable adsorption [28]. Therefore, the increase in q_e resulted from an increase of AO7 concentrations. From Fig. 5, the adsorption capacity of AO7 onto the canola was 24.23 mg/g at 293 K. Even though this amount is not greater than that of other adsorbents, it has other advantages such as cost-effective preparation from natural material. The increase of the adsorption with increasing temperature indicated that the adsorption of AO7 ions onto canola was an endothermic process.

The Langmuir and Freundlich equations were used to fit the isotherm data. The Langmuir adsorption model is represented by its linear form [29] Eq. (3).

$$\frac{C_e}{q_e} = \frac{1}{q_m K_L} + \frac{C_e}{q_m} \quad (3)$$

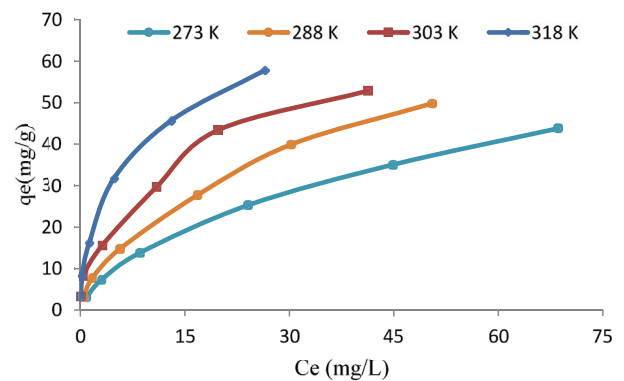


Fig. 5. Adsorption isotherms of the AO7 onto the dried canola at different temperatures.

where C_e (mg/L) is the equilibrium concentration, q_e (mg/g) is the amount of adsorbed adsorbate per unit mass of adsorbent at equilibrium, q_m (mg/g) is adsorption capacity, and K_L (g/L) is the Langmuir constants. The Langmuir adsorption model presumes that interaction between the adsorbate molecules does not occur, and the model explains monolayer adsorption. When C_e/q_e was plotted against C_e , a straight line with slope $1/q_m$ was obtained (Fig. 6). This result indicates that the adsorption of AO7 on canola follows the Langmuir isotherm. This isotherm data were used to estimate the Langmuir constants K_L and q_m , which are shown in Table 2. Another important parameter (R_L), separation factor or equilibrium parameter, is determined from the following equation [30] Eq. (4):

$$R_L = \frac{1}{1 + K_L C_0} \quad (4)$$

where K_L (L/mg) and C_0 (mg/L) represent the Langmuir constant and the initial AO7 concentration, respectively. The adsorption process is irreversible when R_L is 0 and linear when R_L is 1. When R_L is between 0 and 1, the adsorption process is favorable while it is unfavorable when R_L is greater than 1. The R_L values estimated from the Eq. (4) were between 0 and 1, suggesting that the Langmuir adsorption was favorable (Table 2).

The Freundlich isotherm model assumes that different sites with several adsorption energies are involved. Freundlich adsorption equation as following [31] Eq. (5):

$$\log q_e = \frac{1}{n} \log C_e + \log K_F \quad (5)$$

where q_e and C_e are the adsorbed amount at equilibrium (mg/g) and the equilibrium concentration of the AO7, respectively. K_F and n are Freundlich constants. K_F (mg/g(L/mg)^{1/n}) is the adsorption capacity of the adsorbent and n indicates how favorable the adsorption process. It has generally stated the n values that range 2–10 represent good, 1–2 represent moderately difficult, and less than one represents poor adsorption characteristics. The n value from the equation was greater than 2, implying the canola was good adsorbents for the AO7.

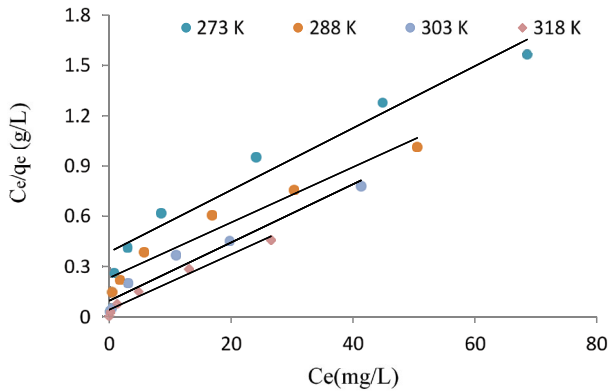


Fig. 6. Langmuir isotherms for the AO7 dye adsorption onto the dried canola at different temperatures.

Table 2

Isotherm parameters for removal of the AO7 by the dried canola at different temperatures

Isotherms	Parameters	Temperatures (K)			
		273	288	303	318
Langmuir	q_e (mg/g)	42.87	45.35	48.73	52.35
	K_L (L/mg)	0.221	0.365	0.545	0.689
	R_L (L/mol)	0.019	0.024	0.031	0.046
	R^2	0.960	0.952	0.956	0.973
Freundlich	K_F (mg/g(L/mg) ^{1/n})	11.2	16.4	19.8	23.71
	n	2.57	2.95	3.34	3.81
	R^2	0.998	0.997	0.989	0.997

The slope $1/n$ plays a role as a scale of adsorption intensity or surface heterogeneity, and the adsorption becomes more heterogeneous as it is closer to zero. The straight line with slope $1/n$ was given from the plot of $\log q_e$ vs. $\log C_e$ which was displayed in Fig. 7. The constants (K_F and n) of the Freundlich model were calculated by Eq. (3) and listed in Table 2 including the Langmuir constants. The adsorption of the AO7 to the dried canola was proven to fit better with the Freundlich isotherm based on the correlation coefficient (Table 2). The amount of maximum monolayer uptake capacity of AO7 dye by canola biomass was obtained at 42.87, 45.35, 48.73, and 52.35 mg/g at temperatures of 273, 288, 303 and 318 K, respectively. This amount has been compared with q_m achieved from the other studies for the removal of AO7 dye. Table 3 shows the maximum uptake capacity from the Langmuir model by various sorbents.

3.3. Adsorption kinetics

Three kinetic models such as pseudo-first-order, pseudo-second-order and intra-particle diffusion models were chosen to elucidate the mechanism and rate-controlling step during the adsorption process. The pseudo-first-order equation is expressed below [41,42]:

$$\log(q_e - q_t) = \log(q_e) - \frac{K_1}{2.303} t \quad (6)$$

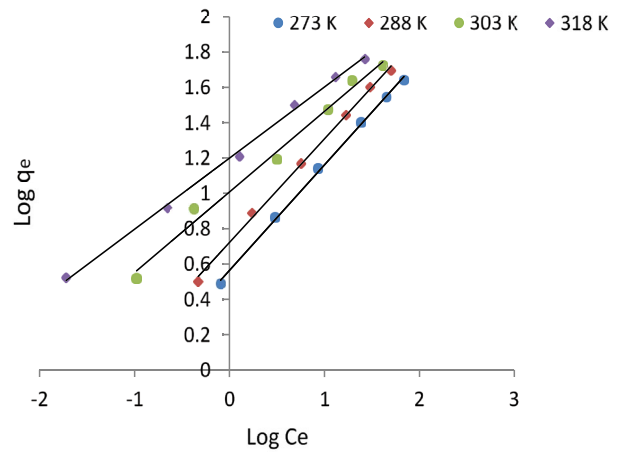


Fig. 7. Freundlich isotherms for the AO7 dye adsorption onto the dried canola at different temperatures.

where q_e (mg/g) is the AO7 adsorption capacity at equilibrium, q_t (mg/g) is the amount of adsorbate removed at time t (min), and K_1 (min⁻¹) is the rate constant of the pseudo-first-order reaction. Fig. 8 illustrated that the q_e and K_1 values can be calculated by the slope and intercept of the plots of $\log(q_e - q_t)$ vs. t . The linear plots of $\log(q_e - q_t)$ vs. t at various concentrations with the correlation coefficients (R^2) higher than 0.932 is a suggestion that adsorption of AO7 on canola predominantly succeeds the pseudo-first-order kinetic model, but the experimental values of $q_{e,exp}$ (mg/g) are nowhere near the calculated $q_{e,cal}$ (mg/g).

The pseudo-second-order kinetic model can be expressed in linear form as follows [43, 44]:

$$\frac{t}{q_t} = \frac{1}{K_2 q_e^2} + \frac{t}{q_e} \quad (7)$$

where K_2 (g/mg min) is the rate constant of the pseudo-second-order reaction. The q_e and K_2 values were estimated from the slope and intercept of plots of t/q_t vs. t which was displayed in Fig. 9. The linear plots of t/q_t vs. t at different concentrations were good with higher correlation coefficients ($R^2 = 0.995$). This implies that AO7 adsorption onto the canola biomass comes behind the pseudo-second-order kinetic model. The good linear plots of t/q_t vs. t at different concentrations with the correlation coefficients (R^2) higher than 0.995 suggest that adsorption of AO7 onto canola biomass fitted better to pseudo-second-order kinetic model. In addition, the calculated data ($q_{e,cal}$) has a remarkable agreement with the experimental data ($q_{e,exp}$). Table 4 showed the kinetic parameters.

The intra-particle-diffusion equation is shown below [45].

$$q_t = Kt^{0.5} + I \quad (8)$$

A model proposed by Weber and Morris, other known as the intra-particle diffusion model proposes that the adsorption mechanism occurs due to the diffusion of adsorbate molecules into the adsorbent pores. The plots of q_t vs. $t^{1/2}$ are

Table 3
Comparison of the maximum uptake of various adsorbent for AO7

Adsorbents	q_e (mg/g)	Ref.	Adsorbents	q_e (mg/g)	Ref.
<i>Cyperus rotundus</i>	19.25	[26]	Granular activated carbons	96.25	[32]
Treated bagasse	144.93	[33]	Bottom ash	3.78	[34]
Untreated bagasse	28.01	[35]	Kenya tea pulps	31.25	[36]
Spent brewery grains	30.47	[37]	Al ₂ O ₃ Nanoparticles	112.8	[38]
<i>Azolla rongpong</i>	76.92	[15]	De-oiled soya	14.36	[34]
Beech wood sawdust	5.06	[39]	Rice stem	27.81	[40]

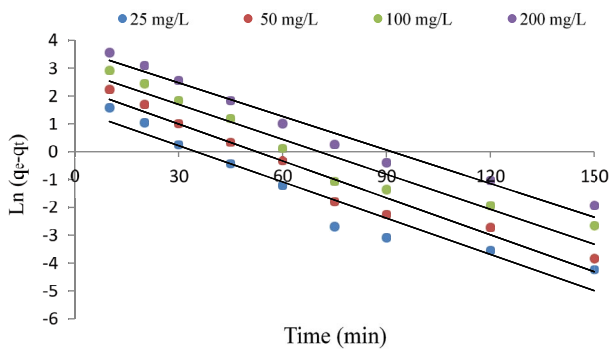


Fig. 8. Pseudo-first-order kinetic plots for the AO7 adsorption onto the dried canola.

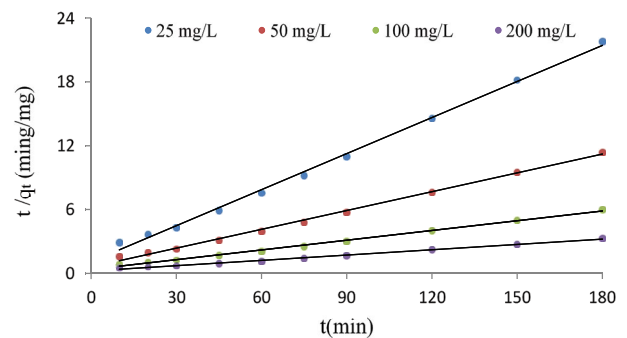


Fig. 9. Pseudo-second-order kinetic plots for the AO7 adsorption onto the dried canola.

in Fig. 10 and the values of K , C , and R^2 are summarized in Table 4. As seen in Fig. 10, all the plots are disseminated in three individual linear segments that indicate three different stages.

The primary stage focuses on the diffusion of AO7 to the external surface of the dried canola or the boundary layer diffusion of adsorbate molecules. The second stage is about the gradual adsorption where the intra-particle diffusion that is, the rate-limiting step. The following stage is allocated to the equilibrium, where the intra-particle diffusion starts to decline because of the extremely low concentration of AO7 leftover in the solution that leads to rather lower K values for each stage. Moreover, both the second and third stages bypass the origin, thus explaining that the rate-limiting step of the adsorption process is not solely governed by intra-particle diffusion [46].

Table 4
Kinetic parameters for AO7 adsorption onto the dried canola

C_0 (mg/L)	Pseudo-second-order model			Pseudo-first-order model			Intra-particle diffusion model		
	K_2 (min ⁻¹)	R^2	q_e (mg/g)	K_1 (min ⁻¹)	R^2	q_e (mg/g)	K	I	R^2
25	0.104	0.996	8.84	0.099	0.973	3.21	0.386	4.08	0.653
50	0.095	0.996	17.24	0.101	0.941	7.64	0.761	7.5	0.674
100	0.0824	0.995	33.33	0.094	0.957	19.39	1.552	13.11	0.696
200	0.0695	0.995	62.5	0.092	0.932	31.36	2.994	21.74	0.713

3.4. Thermodynamic analysis

Effect of temperature on the adsorption of AO7 on the canola was assessed using the free energy change (ΔG°), enthalpy change (ΔH°), and entropy change (ΔS°). To assess the thermodynamic parameters using the following equations [47–49], the Langmuir isotherm was applied:

$$\Delta G^\circ = -RT \ln K \quad (9)$$

$$\ln K = \frac{\Delta S^\circ}{R} - \frac{\Delta H^\circ}{RT} \quad (10)$$

where K , R , and T are the Langmuir equilibrium constant (l/mol), the gas constant (8.314 J/mol K), and the temperature (K), respectively. Table 5 presents the thermodynamic

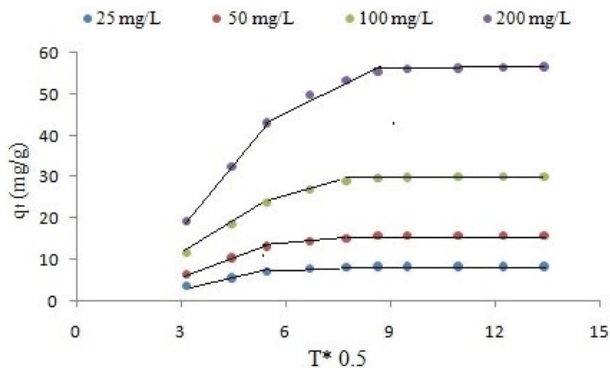


Fig. 10. Intra-particle diffusion plots for adsorption at different initial AO7 concentrations.

Table 5

Thermodynamic parameters for AO7 adsorption on the dried canola

Tem (°K)	ΔG° (kJ/mol)	ΔH° (kJ/mol)	ΔS° (kJ/mol/K)
273	-0.045		
288	-1.198		
303	-2.519	29.62	0.107
318	-4.987		

parameters at different temperatures. The negative values showed confirmation of the possibility of the process and the instantaneous nature of its adsorption. The decrease of ΔG° values with a temperature increase suggests that the adsorption process of AO7 on the dried canola is more apt to higher temperatures. The values assessed from the plot of ΔG° vs. T were 29.62 and 0.107 KJ/mol K of ΔH° and ΔS° , respectively. It was suggested that the ΔH° of physisorption is less than 40 kJ/mol [50,51]. Based on ΔH° , adsorption of AO7 on the canola was regarded as a physisorption process. As the value of ΔH° was positive, the adsorption reaction was regarded as an endothermic process. The positive value of ΔS° reflecting the affinity of the dried canola for AO7 furthermore suggests certain structural changes in dye and the canola residue.

The best kinetic model is the pseudo-second-order model for the adsorption of AO7 on canola. In accordance, the rate constants (K_2) of the pseudo-second-order model were utilized to estimate the activation energy of the adsorption process by applying the equation [52] below:

$$\ln K_2 = \ln K - \frac{E_a}{RT} \quad (11)$$

where K_2 , K , E_a , R , and T are the rate constants of the following respectively: the pseudo-second-order model (g/mg min), the activation energy (kJ/mol), the gas constant (8.314 J/mol K) and temperature (K). The activation energy reached 8.80 kJ/mol at a concentration of 100 mg/L, and the magnitude of activation energy gives information for the type of sorption. The two main types of adsorption are physical and chemical process. Activated chemical adsorption shows that the

rate tends to vary with temperature depending on the finite activation energy (8.4–83.7 kJ/mol) in the relevant equation. The activation energy is close to zero [53,54] in non-activated chemical adsorption. Therefore, ΔH° , ΔG° , and E_a values suggested that adsorption of AO7 on canola was a physisorption process. The positive values of E_a suggested that adsorption may be an endothermic process.

In deionized water, only 24.5% AO7 pre-adsorbed onto canola biomass was desorbed, showing most AO7 to be strongly bond to the canola biomass. With added sodium chloride at 0.1, 0.2 and 0.4 N concentrations, significantly 51.37%, 68.6%, and 84.3% of adsorbed AO7 were released within 90 min. The enhanced AO7 desorption with increasing ionic strength is consistent with the electrostatic interaction mechanism of AO7 adsorption on canola biomass. At high ionic strength, the negatively charged canola biomass and positive charged AO7 would be screened by the respective Na^+ and Cl^- counter ions, breaking their electrostatic bonds and releasing AO7 molecules [55].

4. Conclusion

This investigation was performed for an examination on the equilibrium and dynamic adsorption of AO7 on the dried canola. The adsorption experiments revealed that canola biomass was good efficient in adsorption of AO7 due to high specific surface area (72.5 m²/g). Textural, morphological and surface chemistry characteristics were studied by nitrogen physisorption, BET, ESEM, FT-IR, and XRD. It was evident that the adsorption capacity increased with the increase of temperature. Adsorption data were fitted with the pseudo-first and pseudo-second-order kinetic equations. The best method to describe the sorption kinetics was by the pseudo-second-order kinetic equation. An indication of the thermodynamic analysis states that the adsorption of AO7 dye on canola residual was instantaneous and endothermic. In addition, through a physisorption process, the adsorption of AO7 on the canola residual had occurred.

Acknowledgement

This research was supported by Basic Science Research Program through the National Research Foundation of Korea (NRF) funded by the Ministry of Education (NRF-2019R111A3A01062424). Also we are grateful to the student research committee of Zahedan University of medical sciences for their supports.

References

- [1] G. Crini, Non-conventional low-cost adsorbents for dye removal: a review, *Bioresour. Technol.*, 97 (2006) 1061–1085.
- [2] Y.Safa, H.N. Bhatti, Adsorptive removal of direct textile dyes by low-cost agricultural waste: application of factorial design analysis, *Chem. Eng. J.*, 167 (2011) 35–41.
- [3] M. Joshi, R. Bansal, R. Purwar, Color removal from textile effluents, *Indian J. Fiber Text. Res.*, 29 (2004) 239–259.
- [4] L. Laasri, M.K. Elamrani, O. Cherkaoui, Removal of two cationic dyes from a textile effluent by filtration-adsorption on wood sawdust, *Environ. Sci. Pollut. Res.*, 14 (2007) 237–240.
- [5] Y. Bulut, N.Gozubenli, H. Aydin, Equilibrium and kinetics studies for adsorption of direct blue 71 from aqueous solution by wheat shells, *J. Hazard. Mater.*, 144 (2007) 300–306.

- [6] A. Tor, Y. Cengeloglu, Removal of congo red from aqueous solution by adsorption onto acid-activated red mud, *J. Hazard. Mater.*, 138 (2006) 409–15.
- [7] C.Y. Tan, Li. G, X.Q. Lu, Z. Chen, Biosorption of basic orange using dried *A. filiculoides*, *Ecol. Eng.*, 36 (2010) 1333–1340.
- [8] V.K. Garg, R. Gupta, A.B. Yadav, R. Kumer, Dye removal from aqueous solution by adsorption on treated sawdust, *Bioresour. Technol.*, 89 (2003) 121–124.
- [9] A. Khaled, A.E. Nem, A. El-Sikail, O. Abdelwahab, Removal of Direct N Blue-106 from artificial textile dye effluent using activated carbon from orange peel: adsorption isotherm and kinetic studies, *J. Hazard. Mater.*, 165 (2009) 100–110.
- [10] K.S. Low, C.K. Lee, B.F. Tan, Quaternized wood as a sorbent for reactive dyes, *Appl. Biochem. Biotechnol.*, 87 (2000) 233–245.
- [11] C. Ferdag, A.O. Necip, Biosorption of acidic dyes from aqueous solution by *Paenibacillus macerans*: kinetic, thermodynamic and equilibrium studies, *Chem. Eng. J.*, 150 (2009) 122–130.
- [12] V.K. Garg, R. Kumar, R. Gupta, Removal of malachite green dye from aqueous solution by adsorption using agro-industry waste: a case study of *Prosopis cineraria*, *Dyes Pigm.*, 62 (2004) 1–10.
- [13] P.S. Kumar, S. Ramalingam, C. Senthamarai, M. Niranjana, Adsorption of dye from aqueous solution by cashew nut shell: studies on equilibrium isotherm, kinetics, and thermodynamics of interactions, *Desalination*, 261 (2010) 52–60.
- [14] V. Ponnusami, V. Krithika, R. Madhuran, S.N. Srivastava, Biosorption of reactive dye using acid-treated rice husk: factorial design analysis, *J. Hazard. Mater.*, 142 (2007) 397–403.
- [15] T.V.N. Padmesh, K. Vijayaraghavan, G. Sekaran, M. Velan, Application of *Azolla* rongpong on biosorption of acid red 88, acid green 3, acid orange 7 from synthetic solutions, *Chem. Eng. J.*, 122 (2006) 55–63.
- [16] M.A. Zazouli, A.H. Mahvi, Y. Mahdavi, Isothermic and kinetic modeling of fluoride removal from water by means of the natural biosorbents sorghum and canola, *Fluoride*, 48 (2015) 15–22.
- [17] M.A. Zazouli, D. Balarak, F. Karimnezhad, F. Khosravi, Removal of fluoride from aqueous solution by using of adsorption onto modified *Lemna minor*: adsorption isotherm and kinetics study, *J. Mazandaran Univ. Med. Sci.*, 23 (2014) 208–217.
- [18] M. Dogan, H. Abak, M. Alkan, Biosorption of methylene blue from aqueous solutions by hazelnut shells: equilibrium, parameters, and isotherms, *Water Air Soil Pollut.*, 192 (2008) 141–153.
- [19] D. Balarak, F.K. Mostafapour, Adsorption of acid red 66 dye from aqueous solution by heat-treated rice husk, *Res. J. Chem. Environ.*, 22 (2018) 80–84.
- [20] V.S. Mane, I.D. Mall, Kinetic and equilibrium isotherm studies for the adsorptive removal of brilliant green dye from aqueous solution by rice husk ash, *J. Environ. Manage.*, 84 (2007) 390–400.
- [21] A. Ashori, Y. Hamzeh, E. Azadeh, S. Izadyar, M. Layeghi, M.S. Niaraki, Potential of canola stalk as biosorbent for the removal of remazol black B reactive dye from aqueous solutions, *Wood Chem. Technol.*, 32 (2012) 35–42.
- [22] M.A. Zazouli, J. Yazdani, D. Balarak, M. Ebrahimi, Y. Mahdavi, Removal acid blue 113 from aqueous solution by canola, *J. Mazandaran Univ. Med. Sci.*, 23 (2013) 73–81.
- [23] D. Balarak, Y. Mahdavi, E. Bazrafshan, A.H. Mahvi, Kinetic, isotherms and thermodynamic modeling for adsorption of acid blue 92 from aqueous solution by modified *Azolla filiculoides*, *Fresenius Environ. Bull.*, 25 (2016) 1321–1330.
- [24] A. Sari, M. Tuzen, Biosorption of cadmium(II) from aqueous solution by red algae (*Ceramium virgatum*): equilibrium, kinetic and thermodynamic studies, *J. Hazard. Mater.*, 157 (2008) 448–454.
- [25] S. Chandrasekhar, P.N. Pramada, Rice husk ash as an adsorbent for methylene blue-effect of ashing temperature, *Adsorption*, 12 (2006) 27–43.
- [26] D. Balarak, H. Azarpira, Biosorption of acid orange 7 using dried *Cyperus rotundus*: isotherm studies and error functions, *Int. J. Chem. Technol. Res.*, 9 (2016) 543–549.
- [27] P. Kaushik, A. Malik, Fungal dye decolorization: recent advances and future potential, *Environ. Int.*, 35 (2009) 127–141.
- [28] K. Mohanty, M. Jha, B.C. Meikap, M.N. Biswas, Biosorption of Cr(VI) from aqueous solution by *Eichhornia crassipes*, *Chem. Eng. J.*, 117 (2006) 71–77.
- [29] C. Namasivayam, D. Kavitha, XRD and SEM studies on the mechanism of adsorption of dyes and phenols by coir pith carbon from aqueous phase, *Microchem. J.*, 82 (2006) 43–48.
- [30] F. Colak, N. Atar, A. Olgun, Biosorption of acidic dyes from aqueous solution by *Paenibacillus macerans*: kinetics, thermodynamic and equilibrium studies, *Chem. Eng. J.*, 150 (2009) 122–130.
- [31] R. Gong, Y. Ding, M. Li, C. Yang, H. Liu, Y. Sun, Utilization of powdered peanut hull as biosorbent for removal of anionic dyes from aqueous solution, *Dyes Pigm.*, 64 (2005) 187–192.
- [32] X. Quan, X. Liu, L. Bo, S. Chen, Y. Zhao, X. Cui, Regeneration of acid orange 7-exhausted granular activated carbons with microwave irradiation, *Water Res.*, 38 (2004) 4484–4490.
- [33] N.A. Malek, N.M. Sihat, A.S. Mahmud, Adsorption of acid orange 7 by cetylpyridinium bromide modified sugarcane bagasse, *Jurnal Teknologi (Sci. Eng.)*, 78 (2016) 97–103.
- [34] V.K. Gupta, A. Mittal, V. Gajbe, J. Mittal, Removal and recovery of the hazardous azo dye acid orange 7 through adsorption over waste materials: bottom ash and de-oiled soya, *Ind. Eng. Chem. Res.*, 45 (2006) 1446–1453.
- [35] M.S. Madhav, M. Soni, C.K. Singhal, V. Gautam, Study of operational parameters and kinetics of biosorption of acid orange 7 by untreated sugarcane bagasse, *J. Chem. Pharm. Res.*, 5 (2013) 523–531.
- [36] B. Naraghi, F. Zabihi, M.R. Narooie, M. Saeidi, H. Biglari, Removal of acid orange 7 dye from aqueous solutions by adsorption onto Kenya tea pulps; granulated shape, *Electron. Physician*, 9 (2017) 4312–4321.
- [37] J.P. Silva, S. Sousa, J. Rodrigues, Adsorption of acid orange 7 dye in aqueous solutions by spent brewery grains, *Sep. Purif. Technol.*, 40 (2004) 309–315.
- [38] E. Khosla, S. Kaur, N. Pragnesh, Mechanistic study of adsorption of acid orange-7 over aluminum oxide nanoparticles, *J. Eng.*, 8 (2013) 525–532.
- [39] S. Izadyar, M. Rahimi, Use of beech wood sawdust for adsorption of textile dyes, *Pak. J. Biol. Sci.*, 2007 (10) 287–293.
- [40] R.A. Diyanati, D. Balarak, M. Ghasemi, Survey of efficiency agricultural waste in removal of acid orange 7 (AO7) dyes from aqueous solution: kinetic and equilibrium study, *Iranian J. Health Sci.*, 2 (2014) 51–61.
- [41] R.A. Diyanati, Z. Yousefi, J.Y. Cherati, The ability of *Azolla* and *Lemna minor* biomass for adsorption of phenol from aqueous solutions, *J. Mazandaran Univ. Med. Sci.*, 23 (2013) 17–23.
- [42] O. Gok, A.S. Ozcan, A. Ozcan, Adsorption behavior of a textile dye of reactive blue 19 from aqueous solutions onto modified bentonite, *Appl. Surf. Sci.*, 256 (2010) 5439–5443.
- [43] D. Suna, X. Zhang, Y. Wub, X. Liu, Adsorption of anionic dyes from aqueous solution on fly ash, *J. Hazard. Mater.*, 181 (2010) 335–342.
- [44] A.R. Cestar, E.S. Vieira, G.S. Vieira, L.E. Almeida, The removal of anionic dyes from aqueous solutions in the presence of anionic surfactant using aminopropylsilica—a kinetic study, *J. Hazard. Mater.*, 138 (2006) 133–141.
- [45] R. Han, J. Zhang, P. Han, Y. Wang, Study of equilibrium, kinetic and thermodynamic parameters about methylene blue adsorption onto natural zeolite, *Chem. Eng. J.*, 145 (2009) 496–504.
- [46] M. Toor, B. Jin, Adsorption characteristics, isotherm, kinetics, and diffusion of modified natural bentonite for removing diazo dye, *Chem. Eng. J.*, 187 (2011) 79–88.
- [47] C.H. Wu, Studies of the equilibrium and thermodynamics of the adsorption of Cu²⁺ onto as-produced and modified carbon nanotubes, *J. Colloid Interface Sci.*, 311 (2007) 338–346.
- [48] A. Ozcan, E.M. Oncu, A.S. Ozcan, Kinetics, isotherm and thermodynamic studies of adsorption of acid blue 193 from aqueous solutions onto natural sepiolite, *Colloids Surf., A*, 277 (2006) 90–97.
- [49] M. Kara, H. Yuzer, E. Sabah, M.S. Celik, Adsorption of cobalt from aqueous solutions onto sepiolite, *Water Res.*, 37 (2003) 224–232.

- [50] D. Balarak, J. Jafari, G. Hassani, Y. Mahdavi, I.T. Yagi, S. Agarwal, V.K. Gupta, The use of low-cost adsorbent (canola residues) for the adsorption of methylene blue from aqueous solution: isotherm, kinetic and thermodynamic studies, *Colloids Interface Sci. Commun.*, 7 (2015) 16–19.
- [51] D. Balarak, F.K. Mostafapour, A. Joghataei, Adsorption of acid blue 225 dye by multi-walled carbon nanotubes: determination of equilibrium and kinetics parameters, *Der Pharma Chemica*, 8 (2016) 138–145.
- [52] M. Shirmardi, A.H. Mahvi, B. Hashemzadeh, A. Naeimabadi, G. Hassani, The adsorption of malachite green (MG) as a cationic dye onto functionalized multi-walled carbon nanotubes, *Korean J. Chem. Eng.*, 30 (2013) 1603–1608.
- [53] M.M. Mahmoudi, A. Nadali, H.R.S. Arezoomand, A.H. Mahvi, Adsorption of cationic dye textile wastewater using clinoptilolite: isotherm and kinetic study, *J. Text. Inst.*, 110 (2019) 74–80.
- [54] E. Bazrafshan, F.K. Mostafapour, S. Rahdar, A.H. Mahvi, Equilibrium and thermodynamics studies for decolorization of reactive black 5 (RB5) by adsorption onto MWCNTs, *Desal. Water Treat.*, 54 (2015) 2241–2251.
- [55] N.M. Mahmoodi, M. Arami, H. Bahrami, S. Khorramfar, Novel biosorbent (canola hull): Surface characterization and dye removal ability at different cationic dye concentrations, *Desalination*, 264 (2010) 134–142.